Effect of Rayleigh-scattering distributed feedback on multiwavelength Raman fiber laser generation

A. E. El-Taher[*a], P. Harper [a], S. A. Babin[b], D. V. Churkin[b],

E. V. Podivilov[b], J. D. Ania-Castanon[c], S. K. Turitsyn[a]

[a] Photonics Research Group, Aston University, Birmingham, B4 7ET, UK;
[b] Institute of Automation and Electrometry, SB RAS, Novosibirsk 630090, Russia;
[c] Instituto de Óptica, CSIC, C/ Serrano 121, Madrid 28006, Spain

ABSTRACT

We experimentally demonstrate a Raman fiber laser based on multiple point-action fiber Bragg grating (FBG) reflectors and distributed feedback via Rayleigh scattering in a ~22 km long optical fiber. Twenty two lasing lines with spacing of ~100 GHz (close to ITU grid) in C-band are generated at Watts power level. In contrast to the normal cavity with competition between laser lines, the random distributed feedback cavity exhibits highly stable multiwavelength generation with a power-equalized uniform distribution which is almost independent on power. The current set up showing the capability of generating Raman gain of about 100-nm wide giving the possibility of multiwavelength generation at different bands.

Keywords: fiber lasers; Rayleigh scattering; Raman scattering; random lasers.

1. INTRODUCTION

Multiwavelength fiber lasers have attracted great interest due to their wide applications in wavelength division multiplexing (WDM) systems, instrument testing, optical fiber sensors, and spectroscopy. Several techniques have been proposed to ensure stable multi-wavelength laser operation based on semiconductor optical amplifiers[1], erbium-doped fiber lasers[2], spectrum sliced supercontinuum[3] or Raman fiber lasers (RFLs)[4-10].

RFL-based multiwavelength sources are very attractive because of their broad and flat gain at many customizable wavelengths, besides working at room temperature with high output power. Different types of multiwavelength RFLs, mainly in ring cavity configurations, have been proposed and demonstrated utilizing multi-channel filters based on Fabry-Perot[4-6] or Sagnac[7] interferometers. As a result, multi-wavelength RFLs can emit up to 58 stable lines simultaneously with 100 or 50 GHz spacing[4] in different spectral bands[7]. Fiber Bragg gratings (FBGs) reflecting several wavelengths being either multimode[8], phase-shifted[9] or sampled[10] have also been demonstrated for multi-wavelength operation in RFLs with linear cavities but, generally with a relatively low number of spectral lines.

The basic principles of operation of such multiwavelength RFLs is however still rather uncertain. Simple explanations like inhomogeneous saturation of the Raman gain spectrum contradict the direct measurements of the gain saturation that appears homogeneous within a selected Raman gain component[11]. The mechanism of inhomogeneity is shown to be defined by nonlinear effects, namely by four wave mixing (FWM) between generated spectral components either inter-channel (between generated lines) or intra-channel (between longitudinal cavity modes within one line). Since the integral (over frequency) effect of FWM is zero, it leads to a redistribution of power from central to weak side components. This FWM-induced spectral inhomogeneity was initially attributed to inhomogeneous losses[5,6] and then to inhomogeneous gain[12] that is shown to be more correct in the frame of the developed statistical model of multiple FWM interactions. Though the classification of inhomogeneity is a rather academic problem, the main common conclusion[5,6,12] is that the integral FWM-

---

* eltaheae@aston.ac.uk

induced losses depend on the line intensity and spectral width of the line-selecting filter/reflector. Such nonlinear losses result both in spectral broadening of the individual line and in power equalization between the lines at multiwavelength operation.

Note that all multiwavelength RFL schemes[4-10] are based on long fibers (4-50 km), so Rayleigh scattering (RS) accumulated over a long distance and amplified via the Raman effect, may play an important role in such systems. A stable narrow-linewidth lasing utilising RS-based random distributed feedback only (without any regular reflector) has been demonstrated recently[13]. A distributed RS mirror has also been used to improve generation of Brillouin combs in a linear RFL cavity, see e.g.[14,15]. Similarly, it may be utilized as a broadband mirror in multiwavelength RFLs. So, CW generation of five lines has been obtained in the cavity formed by RS mirror and five FBGs separated by 5-10nm[16]. Stable operation with ~1nm separation between the lines appears possible in schemes involving a photonic crystal fiber loop mirror[17] or two different-wavelength FBGs placed at opposite ends of a 200-km long fiber[18].

In this paper we explore an opportunity to achieve stable uniform generation of multiple lines with 0.8-nm spacing (close to ITU 100GHz grid) in a cavity formed by broadband RS-based distributed mirror and an array of FBGs in a simple linear scheme. To make clear the specifics of the random distributed feedback (RDFB) we perform a direct comparison with a laser based on broadband 4% reflection from the cleaved fiber end.

2. EXPERIMENTAL SETUP

The experimental setup is schematically illustrated in Fig. 1. A single pump laser at 1455 nm is coupled into the fiber span through a 1450/1550-nm WDM coupler. The pump wave induces broad Raman gain in the 1550nm C-band region. The Raman gain coefficient depends on the fiber type and has a typical value of ~1/(W*km). The laser cavity is formed by RDFB owing to the Raman amplified Rayleigh backscattering along the fiber, and an array of twenty two highly reflective FBGs placed at the left fiber end. The FBGs have a 3-dB reflection bandwidth of 0.3 nm and their reflection maxima are almost identical, of the order of 94-97%, separated from each other by ~0.8 nm (~100 GHz), so the array covers the wavelength range of 1552-1570 nm. We have paid particular attention to avoid any parasitic feedback from the fiber ends and connections by using angled fiber end facets and angled polished connectors to eliminate 4% Fresnel reflection and spliced fiber spans. A splitter with 1% monitor port was inserted near the right fiber end to measure the Raman laser output power while a four port splitter was inserted near the FBGs to monitor the spectra after the fiber spans and the spectra reflected from the FBGs; spectra measured with a high resolution (~0.01 nm) optical spectrum analyzer (OSA).
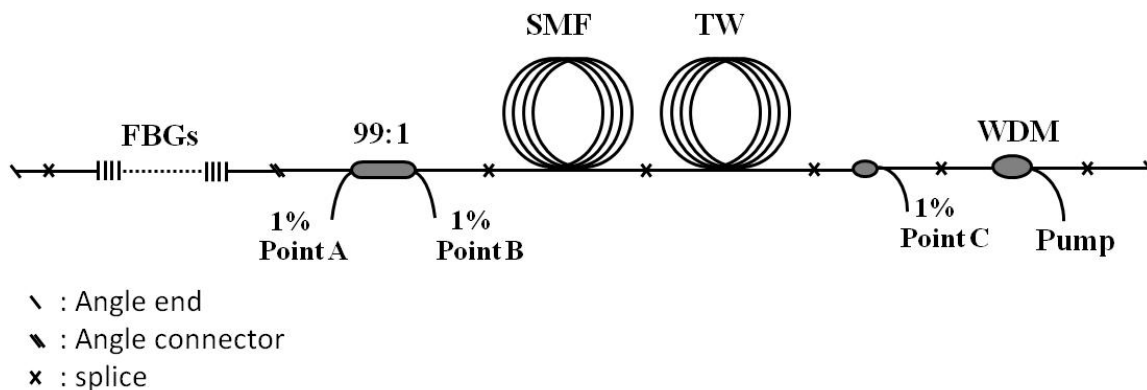

Fig. 1: Schematic depiction of the experimental set-up.

For power-equalized multiwavelength operation one should first flatten the Raman gain spectral profile, because it is known to have two maxima with up to ~10 dB contrast. Usually, multiwavelength pumping is used to reduce gain variance over the spectrum; we have used another approach to solve this problem: the cavity is formed by fibers of

different types - 11 km of SMF-28 and 10.5 km of TrueWave (TW) fibers with Raman gain coefficients 0.38 and 0.593 (*1/W km), correspondingly[19]. In highly nonlinear TW fiber having zero-dispersion wavelength near 1456nm, the 1455nm pump wave is significantly broadened[20], see Fig.2. The broadband pump results in a smoothed Raman gain spectrum with variation less than 3 dB in the 1550-1570 nm wavelength range at pump powers 0.9 - 2.75 W, see inset in Fig. 2. The spectrum in pure SMF having ~10 dB non-uniformity is also shown for comparison.
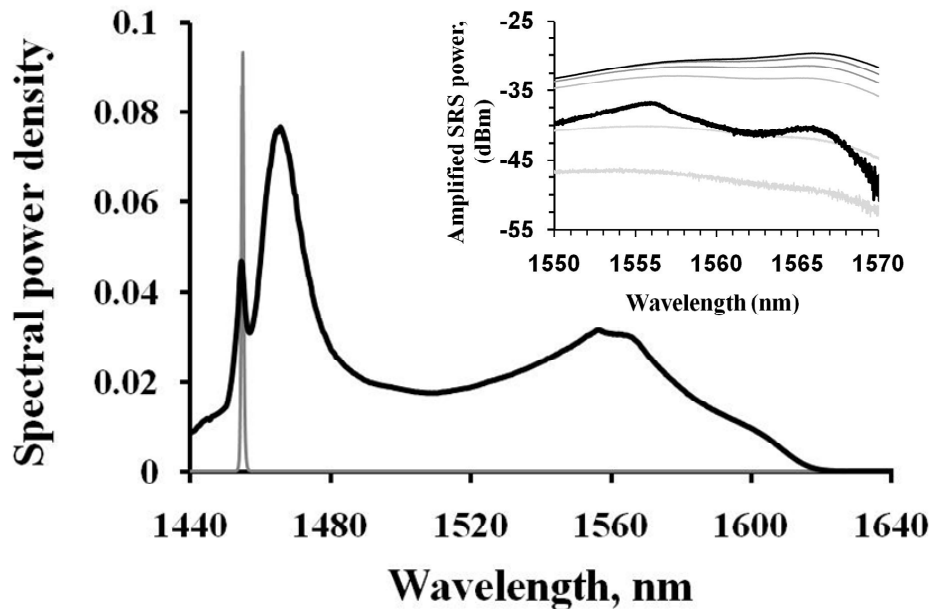

Figutre 2. Comparison between pump power spectrum in linear scale before (grey line) and after (black line) TW fiber at 1.8 W pump power. Inset: The backward measured amplified SRS (FBGs are not installed) as the pump power is increased from 0.9 to 2.75 W for TW and SMF fibers spliced together, and thick black line is the same for SMF fiber of equivalent length, 22km, at 1.8 W.

3. MULTIWAVELENGTH GENERATION

The setup exhibits clear laser behaviour with a threshold pump power of ~0.8 W, Fig. 3. The total output power from the right fiber end can be as high as 1.6 W demonstrating more than 40% generation efficiency. The power variations are small both for the total power as well as for the individual laser lines. The laser simultaneously delivers stable laser radiation at all the twenty two FBG wavelengths (Fig.4a) starting from the threshold (Fig.5a) up to the maximum power (Fig.5b) with background ASE suppression of ~25 dB. The distribution follows the Raman gain curve with two maxima at ~1555 and ~1565 nm and small dip between them. With increasing power only limited change in the spectral shape was observed: there was a relative increase of the long-wavelength range and a decrease of the generated comb contrast from ~15 to ~10 dB on average.

To justify a role of the RS-based random distributed feedback, we arrange a conventional linear cavity between highly reflective FBGs and 4% Fresnel reflection inserted by means of flat cleaving of the fiber end. As expected, the generation threshold for this cavity is lower, see Fig.3 (circles), because of the much higher reflection providing higher cavity Q-factor. However, the slope efficiency for the flat end is lower, thus the highest achievable output power is slightly lower than that for the pure RDFB cavity with angle end.
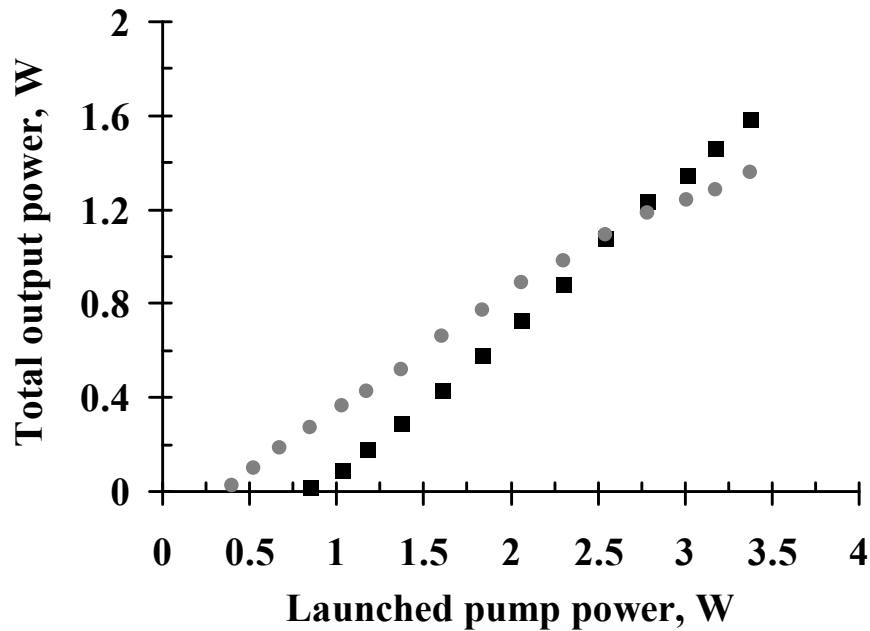
Figure 3. Laser output power as a function of pump power: squares are the output power values for the angle end and circles are the output power values with the flat end.
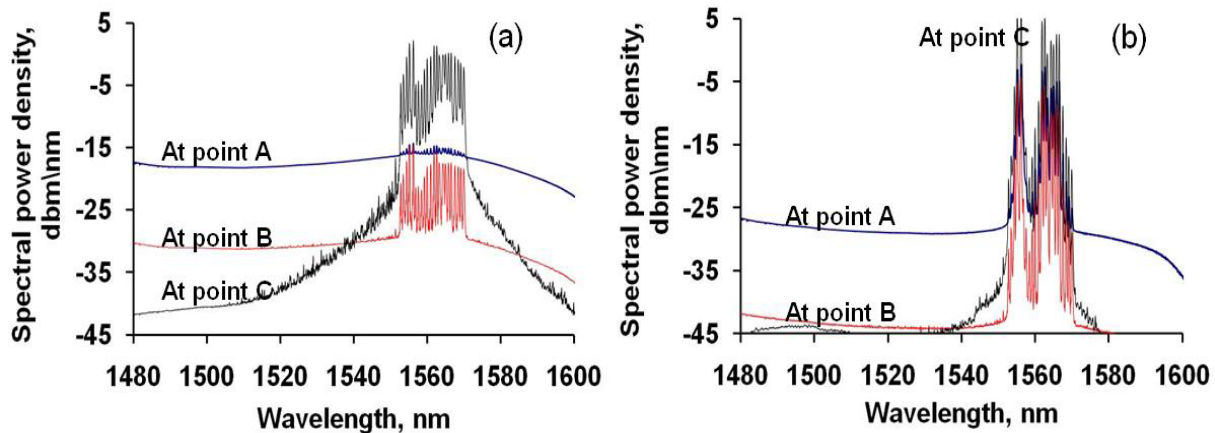

Figure 4. Comparison between the spectra measured at three points for angle end setup (a), and flat-end setup (b). At point A the spectra are measured after the fiber spans, at point B the measured spectra are reflected from the FBGs and at point C the output spactra are measured at the right end of the cavity.

For better understanding of the difference between the two cavities, the spectra are measured at three different points. Point A - to measure the spectra just after the fiber sapns, point B - to measure spectra reflected from the FBGs and point C - to measure the spectra at the right output. Figure 4 showing the spectra measured at the three points for the two cavities at the same power. From figure 4a, for the angle end cavities, the spectra measured after the fiber spans, at point A, showing a gain covering the range for more than 100 nm and on top of it we can see some signals corresponding to FBGs. The FBG's will reflect only the signals corresponding their reflection profile as seen from the spectra measured at

point B the same figure, and the reflected signals are amplified when passed through the fiber again from left to right end with the assistance of the Raman gain caused by the pump light to give a very high signals power at the right output as measured at point C. On the other hand for the set-up with flat end where we have a normal cavity formed by the ~4% reflection from the fiber end and the FBGs, see figure 4b, the spectra at both sides of the fiber, at points A and C, are comparable and we have a high signal level after the fiber on the left side while output signal at the right side is lower (in average) than that for angle end setup. Note that the FBG's used in that experiment covered only the range 1552-1570nm, however, if we change to any other band or increase the number of FBGs. we expect the same results.

In addition, the generation spectra measured with a flat end cavity reveal non-uniform distributions strongly changing with power, see Fig.5 (grey curves). At low pump power, the output spectrum consists of two different groups of lines generated near the Raman gain spectral maxima, see Fig.5a. The generation at wavelengths near the local minimum is suppressed, contrary to the case of RDFB cavity with angle ends. With increasing pumping the power maximum shifts to longer wavelengths owing to the effect of cascaded Raman scattering (between the lines) discussed earlie[5]. The distribution becomes flatter but less uniform: the difference between line intensities is >30 dB, which is much greater than that for RDFB cavity, whereas the comb contrast is similar (~10 dB). At the same time, the ASE suppression is greater than 40 dB.
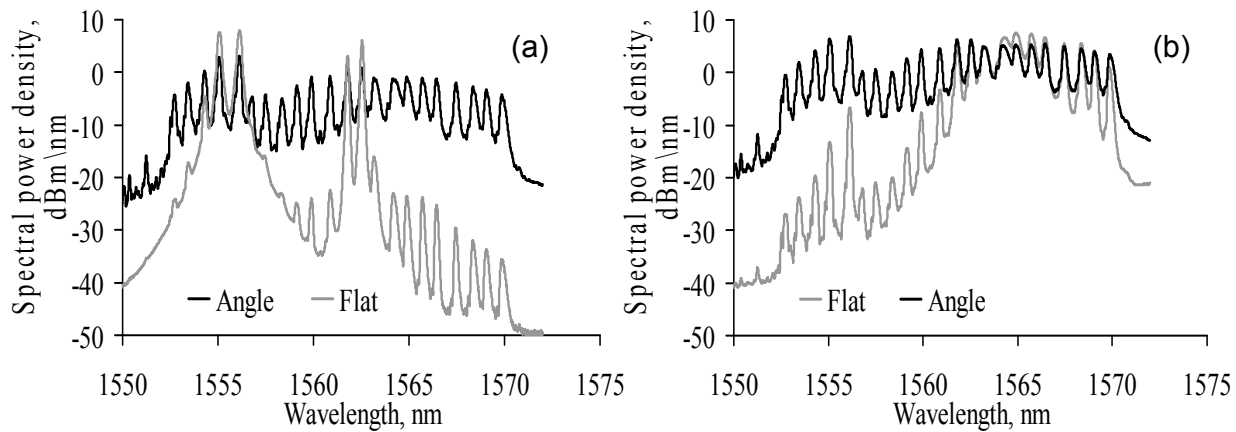

Figure 5. Optical spectra at various output power for both angle (black) and flat (grey) end setups: (a) at 0.28W, (b) at 1.35W.
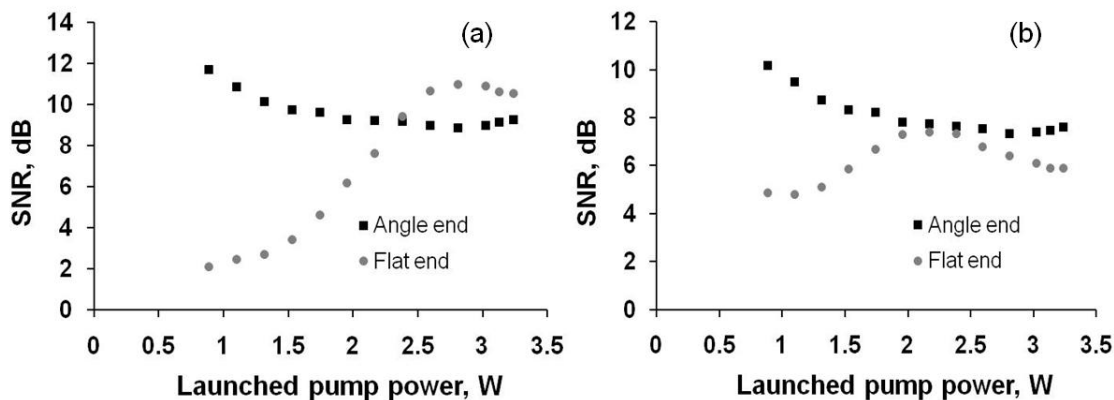

Figure 6. Comparison between the variation of SNR for the grid as a function of launched pump power for both cavities for two different channels: (a) for channel 2, (b) for channel 8.

Figure 6 shows the variation of signal to noise ratio (SNR) in the grid as function of pump power for two different channels for both cavities, which clearly demonstrate that for the flat-end cavity the power level for each channel is strongly changing with increasing input power and also is changing differently for different channels, while for the angle end cavity, the power for all channels increased uniformly as we increase the input power with some decrease of SNR. The difference of SNR for each channels depends on the exact separation between the FBGs central wavelengths.

The mechanisms responsible for the observed RDFB effects in multi-wavelength Raman lasers can be considered as follows. Firstly, the experimentally proved much better power equalization between the generated lines in the RDFB cavity is certainly defined by unique features of RS-based random distributed feedback: A spectral selectivity with near-Gaussian statistics[21] at absence of the longitudinal modes[13]. In a conventional cavity, the modes formed by point reflectors (e.g. FBG and 4% facet) have equidistant frequencies and a more-or-less uniform power distribution along the fiber cavity, thus leading to competition between the modes utilizing the same pump (this is also true for different lines), whereas in the pure RDFB laser the generated radiation is random in frequency and space. One can define only the average longitudinal distribution of such "random modes" that is mainly defined by the Raman gain (pump power)[13]. We suppose that at multiwavelength operation of the RDFB laser, the different lines may have a sufficiently different distribution along the fiber to reduce their competition self-consistently.

The second important fact is that the total power of the pure RDFB cavity becomes equal and even slightly higher than that for normal cavity, in spite of higher linear losses. The reasons are supposed to deal with nonlinear losses. As the fiber length of ~22 km is close to the estimated length of distributed RS mirror[13] the RDFB effect on generation becomes comparable with the Fresnel reflection at high Raman gain that defines high efficiency of lasing. At nearly equal output power, a variation of power along the fiber is quite different in two cases: in case of pure RDFB the power at the left end is much lower than that for the 4% reflection that means lower nonlinear losses on FBGs. The effect is stronger for the lines with higher power that is important in the non-equalized case. We have directly measured the output power and spectra at the left end confirming much higher intensity and corresponding nonlinear losses at the FBGs in case of the Fresnel cavity. The lost power is close to the observed difference in the output power. Some input to the total power can also be accounted for the different ASE background. Note that the cascaded Raman shift is defined by intensity integral along the fiber that is larger for the 4% cavity. For quantitative analysis of the effects, numerical simulations of the spatial distributions in both cases are needed

Since the effect of RDFB is important in a normal cavity, as shown here for Fresnel reflection, it may also have an impact on power equalization in other multi-wavelength RFLs with long cavities[4-10]. Note that similar effect was observed for a Brillouin comb which becomes uniform with the assistance of RS at high pump power[15].

4. CONCLUSIONS

In conclusion, we have shown that CW multi-wavelength generation with 40% efficiency is easily achieved in telecommunication fiber owing to the random distributed Rayleigh scattering feedback. The power in all lines is equalized in correspondence with a Raman gain spectrum flattened by means of the pump spectral broadening. The rest non-uniformity can be eliminated by optimizing the FBGs reflectivity, which is not possible in schemes with loop mirrors and interferometers. The number of generated lines is limited in our case by the number of available FBGs; however, the current set up is able to produce a gain which cover a range of ~100 nm, so we anticipate that the number of lines can be easily increased by using additional FBGs. This technique can also be applied for other spectral bands using corresponding pump and FBGs wavelength where the power at each line will depend on the strength of the corresponding FBG mainly but not on the Raman gain. The proposed multiwavelength Raman fiber laser has potential uses in telecommunications and sensing.

REFERENCES

[1] N. Pleros, C. Bintjas, M. Kalyvas, G. Theophilopoulos, K. Yiannopoulos, S. Sygletos, and H. Avramopoulos, "Multiwavelength and power equalized SOA laser sources", IEEE Photon. Technol. Lett. 14, 693-695 (2002).

[2] A. Bellemare, M. Karasek, M. Rochette, S. L. Rochelle, and M. Tetu, "Room temperature multifrequency erbium-doped fiber lasers anchored on the ITU frequency grid," J. Lightwave Technol. 18, 825-831 (2000).

[3] Futami, F. Kikuchi, K., Low-noise multiwavelength transmitter using spectrum-sliced supercontinuum generated from a normal group-velocity dispersion fiber, IEEE Photon. Technol. Lett., 13, 73-75 (2001).

[4] N.S. Kim, X. Zou, "CW depolarized multiwavelength Raman fiber ring laser with over 58 channels and 50 GHz channel spacing," in OFC 2002 Proc., 640-641 (2002).

[5] Q. Wang, Y. Wang, W. Zhang, X. Feng, X. Liu, and B. Zhou, "Inhomogeneous loss mechanism in multiwavelength fiber Raman ring lasers", Opt. Lett. 30, 952-954 (2005).

[6] Q. Wang, X. Liu, L. Xing, X. Feng, and B. Zhou, "Experimental investigation of an inhomogeneous loss and its influence on multiwavelength fiber lasers", Opt. Lett. 30, 3033-3035 (2005).

[7] C.-S. Kim, R.M Sova, J.U. Kang, "Tunable multi-wavelength all-fiber Raman source using fiber Sagnac loop filter", Opt. Comm. 218, 291-295 (2003).

[8] Y. Han, S. B. Lee, D. S. Moon, and Y. Chung, "Investigation of a multiwavelength Raman fiber laser based on few-mode fiber Bragg gratings", Opt. Lett. 30, 2200-2 (2005).

[9] Y.-G. Han, T. V. A. Tran, S.-H. Kim, and S. B. Lee, "Development of a multiwavelength Raman fiber laser based on phase-shifted fiber Bragg gratings for long-distance remote-sensing applications", Opt. Lett. 30, 1114-1116 (2005).

[10] Z. Wang, Y. Cui, B, Yun, and C. Lu, "Multiwavelength generation in a Raman fiber laser with sampled Bragg grating", IEEE Photon. Tech. Lett. 17, 2044-2046 (2005).

[11] S.A. Babin, D.V. Churkin, S.I. Kablukov, E.V. Podivilov. "Raman gain saturation at high pump and Stokes powers", Optics Express 13, 6079–6084 (2005).

[12] S. A. Babin, D. V. Churkin, A. E. Ismagulov, S. I. Kablukov and E. V. Podivilov, "FWM-induced turbulent spectral broadening in a long Raman fiber laser", JOSA B 24, 1729-1738 (2007).

[13] S. K. Turitsyn, S. A. Babin, A. E. El-Taher, P. Harper, D. V. Churkin, S. I. Kablukov, J. D. Ania-Castañón, V. Karalekas, E. V. Podivilov, "Random distributed feedback fibre laser", Nature Photonics 4, 231-235 (2010).

[14] A. K. Zamzuri, M. I. Md. Ali, A. Ahmad, and R. Mohamad, "Brillouin–Raman comb fiber laser with cooperative Rayleigh scattering in a linear cavity", Opt. Lett. 31, 918-920 (2006).

[15] A. K. Zamzuri, M. H. Al-Mansoori, N. Md. Samsuri, and M. A. Mahdi, "Contribution of Rayleigh scattering on Brillouin comb line generation in Raman fiber laser", Appl. Opt. 49, 3506-3510 (2010).

[16] O. Frazão, C. Correia, J.L. Santos, and J.M. Baptista, "Raman fibre Bragg-grating laser sensor with cooperative Rayleigh scattering for strain–temperature measurement," Meas. Sci. Technol. 20, 045203 (2009).

[17] A.M.R. Pinto, O. Frazão, J.L. Santos, M. Lopez-Amo, " Multiwavelength fiber laser based on a photonic crystal fiber loop mirror with cooperative Rayleigh scattering," Appl. Phys. B 99, 391-395 (2010).

[18] A. E. El-Taher, M. Alcon-Camas, S. A. Babin, P. Harper, J. D. Ania-Castañón, and S. K. Turitsyn, "Dual-wavelength, ultralong Raman laser with Rayleigh-scattering feedback," Opt. Lett. 35, 1100-1102 (2010).

[19] C. Fludger, A. Maroney, N. Jolley, R. Mears, "An analysis of the improvements in OSNR from distributed Raman amplifiers using modern transmission fibers," OFC Conference. Vol.37. Opt. Soc. America., DC, USA, Part 4, 100-102 (2000).

[20] T. J. Ellingham et al., "Enhanced Raman amplifier flatness with nonlinear broadening over non-standard transmission fibre," Opt. Commun. 257, 176-179 (2006).

[21] A. A. Fotiadi, R. V. Kiyan, "Cooperative stimulated Brillouin and Rayleigh backscattering process in optical fiber," Opt. Lett. 23, 1805-1807 (1998).